Neutral Ligands for Selective Chloride Anion Complexation: (α,α,α,α)-5,10,15,20-Tetrakis(2-(arylurea)phenyl)porphyrins

Raymond C. Jagessar,[†] Maoyu Shang,[‡] W. Robert Scheidt,*[,‡] and Dennis H. Burns*[,†]

Contribution from the Department of Chemistry, Wichita State University, Wichita, Kansas 67260, and Department of Chemistry and Biochemistry, University of Notre Dame, Notre Dame, Indiana 46556

Received June 12, 1998

Abstract: A series of neutral, urea-appended, free-base porphyrins and their Zn(II) complexes have been synthesized and characterized. The (α,α,α,α)-5,10,15,20-tetrakis(2-(arylurea)phenyl)porphyrins bind strongly (K (M^{-1}) > 10^3−10^5) to chloride anion in DMSO-d_6 and also in the more competitive solvent system DMSO-d_6/D_2O (88:12, v/v) and bromide anion in DMSO-d_6, as revealed by ^1H NMR titration studies. The porphyrin derivatives exhibited significant binding selectivity since they complexed with the spherical Cl^- and Br^- to a much greater extent than with the tetrahedral $H_2PO_4^-$ and HSO_4^- and the trigonal NO_3^- anions in DMSO-d_6. Indeed, the selectivity trend Cl^- > Br^- ≫ $H_2PO_4^-$ > HSO_4^- > NO_3^- is novel for any neutral urea-anion binding system. On the other hand, the corresponding metalloporphyrins exhibited a decrease in binding strength and selectivity in DMSO-d_6. The stoichiometry of binding for the anions and porphyrins was determined to be 1:1. The enthalpy of complexation was determined to be highly favorable and the entropy of complexation determined to be unfavorable from a variable-temperature ^1H NMR experiment with a 1:1 tetrabutylammonium bromide/porphyrin complex. X-ray crystallography revealed (α,α,α,α)-5,10,15,20-tetrakis(2-(4-chlorophenylurea)phenyl)porphyrin to be the first coordination complex of an anion (chloride and bromide) bound by a neutral free-base porphyrin. The binding motif consisted of the halide, buried deep within the porphyrin pocket, bound by two adjacent urea functional groups via four hydrogen bonds, with the two remaining urea functional groups involved in hydrogen bonding to solvent molecules. The crystal structure of the tetrabutylammonium halide−porphyrin complex showed additional Coulombic interaction between the electron-poor sulfur of a pocket-bound, hydrogen-bonded DMSO and halide anion.

Introduction

The design and fabrication of abiotic supramolecular receptors for anion recognition is an area of much current activity.[1] Particularly challenging is the preparation of receptors that exhibit a high degree of discrimination toward specific anions. Nature, as exemplified by the phosphate and sulfate binding proteins, has surmounted this difficulty by complexing anions exclusively via hydrogen bonding, with selectivity ratios of phosphate over sulfate, or sulfate over phosphate, greater than 10^5.[2] Abiotic hosts that utilize hydrogen-bonding motifs potentially combine the benefits of electroneutrality with directional Coulombic interactions. Thus, functional groups capable of H bonding, when positioned correctly in the supramolecular matrix, would be able to differentiate between the three-dimensional shapes (linear, trigonal, tetrahedral, or spherical) of anions. The anion selectivity would be amplified with the addition of functional groups containing H bonds capable of forming bi- and trifurcated bonding arrays.

However, there are only a few reported preparations of neutral abiotic anion receptors capable of achieving selective recognition, and those that do employ H-bonding motifs bind most strongly to phosphate and carboxylate anions.[3] Especially lacking in the arsenal of anion receptors are those capable of the selective recognition of the chloride anion. The recognition of the chloride anion is a very significant event in biological systems as the first step in its ion transport. Chloride ion channels are critical to respiration, with their facilitated exchange of chloride for bicarbonate anions in erythrocytes.[4] Chloride ion channels also are essential to the modulation of the central

* To whom correspondence should be addressed (D.H.B.). E-mail: burns@wsuhub.uc.twsu.edu.

[†] Wichita State University.

[‡] University of Notre Dame.

(1) For recent reviews, see: (a) Schmidtchen, F. P.; Berger, M. *Chem. Rev.* **1997**, 1609−1646. (b) Beer, P. D. *J. Chem. Soc., Chem. Commun.* **1996**, 689−696. (c) Scheerder, J.; Engberson, J. F. J.; Reinhoudth, D. N. *Recl. Trav. Chim. Pays-Bas* **1996**, *115*, 307−320. (d) Lehn, J.-M. *Supramolecular Chemistry*; VCH: Weinheim, 1995. (e) Izatt, R. M.; Pawlak, K.; Bradshaw, J. S. *Chem. Rev.* **1995**, *95*, 2529−2586. (f) Dietrich, B. *Pure Appl. Chem.* **1993**, *65*, 1457−1464.

(2) (a) Pflugrath, J. W.; Quiocho, F. A. *Nature* **1985**, *314*, 257. (b) He, J. J.; Quiocho, F. A. *Science* **1991**, *251*, 1479. (c) Luecke, H.; Quiocho, F. A. *Nature*, **1990**, *347*, 402. (d) Kanyo, Z. F.; Christianson, D. W. *J. Biol. Chem.* **1991**, *266*, 4264.

(3) (a) Bühlmann, P.; Nishizawa, S.; Xiao, K. P.; Umezawa, Y. *Tetrahedron* **1997**, *53*, 1647−1654. (b) Cameron, B. R.; Loeb, S. J. *J. Chem. Soc., Chem. Commun.* **1997**, 573−574. (c) Beer, P. D.; Graydon, A. R.; Johnson, A. O. M.; Smith, D. K. *Inorg. Chem.* **1997**, *36*, 2112−2118. (d) Nishizawa, S.; Bühlmann, P.; Iwao, M.; Umezawa, Y. *Tetrahedron Lett.* **1995**, *36*, 6483−6486. (e) Scheerder, J.; Engbersen, J. F. J.; Casnati, A.; Ungaro, R.; Reinhoudt, D. N. *J. Org. Chem.* **1995**, *60*, 6448−6454. (f) Scheerder, J.; Fochi, M.; Engbersen, J. F. J.; Reinhoudt, D. N. *J. Org. Chem.* **1994**, *59*, 7815−7820. (g) Kelly, T. R.; Kim, M. H. *J. Am. Chem. Soc.* **1994**, *116*, 7072−7080. (h) Boerrigter, H.; Grave, L.; Nissink, J. W. M.; Chrisstoffels, L. A. J.; van der Mass, J. H.; Verboom, W.; de Jong, F.; Reinhoudt, D. N. *J. Org. Chem.* **1998**, *63*, 4174−4180.

(4) Stryer, L. *Biochemistry*; W. H. Freeman: New York, 1988; Chapter 37.

(5) (a) Koo, Y. H.; Delannoy, M.; Pedersen. P. L. *Biochemistry* **1997**, *36*, 5053- 5064. (b) Hanrahan, J. W.; Tabcharani, J. A.; Becq, F.; Mathews, C. J.; Augustinas, O.; Jensen, T. J.; Chang, X.-B.; Riordan, J. R. *Function and Dysfunction of the CFTR Chloride Channel in Ion Channels and Genetic Diseases*; Dawson, D. C., Frizzel, R. A., Eds.; The Rockefeller University Press: New York, 1995.

10.1021/ja982052i CCC: $15.00
Published on Web 10/29/1998

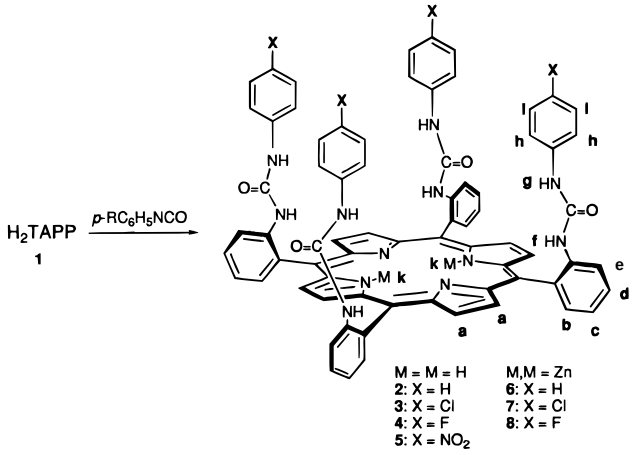

Figure 1. Urea-appended porphyrin illustrating labeled protons of interest.

nervous system through the hyperpolarization of neuronal membranes.[4] Additionally, a mutated chloride channel protein has been implicated as the causative factor of the genetic disease cystic fibrosis.[5] Model systems undoubtedly will prove useful in elucidating the mechanism of transport of chloride across membranes, and of utmost importance will be their ability to discriminate for the chloride anion.

We have recently communicated preliminary (phosphate, nitrate, and chloride) anion coordination studies in DMSO of superstructured porphyrins (**2**−**4**, Figure 1) functionalized with hydrogen-bonding urea moieties.[6] These macrocycles are the first example of a class of neutral, free-base porphyrins that can bind anions and have been demonstrated to be selective chloride anion receptors in a highly competitive solvent. For comparison, the expanded porphyrins can bind anions only when protonated and, thus, exhibit modest anion selectivity due to nondirectional Coulombic interactions[3e] (for example, sapphyrin binds phosphate and fluoride ions with similar binding constants in methanol[7]). Cobaltocenium- and ferrocene-appended porphyrins have recently been reported that exhibit anion binding.[1b,8] The former system requires the combination of the positively charged cobalticinium center and amide hydrogen-bonding environment for anion complexation, whereas neutral ferrocene amide atropisomeric porphyrins do not complex anions unless metalated. Both systems show little anion selectivity (no better than 4:1 binding selectivity between halides, nitrate, and sulfate ions in acetonitrile and dichloromethane, respectively). While anion receptors incorporating the positively charged centers as the main ingredients for anion complexation have been extensively employed by several groups,[1] the preparation of neutral abiotic anion receptors that exhibit selective and exceptionally strong anion complexation is scarce.

An important feature of supramolecules **2**−**4** is the cylindrical orientation of the urea groups on the porphyrin scaffolding that allow **2**−**4** to exhibit remarkable selectivity in their recognition of the spherical chloride anion over that of the trigonal nitrate or tetrahedral phosphate anions. In fact, porphyrins **2**−**4** recognize chloride anion in DMSO with a selectivity of 1000:1 compared to nitrate or 280:1 compared to phosphate anions. Furthermore, electronic tuning via the addition of electronegative substituents (chloro and fluoro) to the para position of the phenyl rings of **3** and **4** allow for some modulation of the supramolecule's anion binding strength and selectivity. In this paper, we fully detail the synthesis and characterization of porphyrins **2**−**8**, including the X-ray crystal characterizations of **7**, and **3** complexed with bromide and chloride anion, a van't Hoff analysis of **4** with bromide anion, and have enlarged the number of binding studies to include more porphyrins (**5**, **6**, and **8**), more anions (Br^-, HSO_4^-), and a more competitive DMSO-d_6/D_2O solvent system.

Results and Discussion

Receptor Synthesis. The synthesis of 5,10,15,20-*meso*-tetrakis(*o*-aminophenyl)porphyrin (H_2TAPP, **1**) was accomplished using the method of Collman,[9] from which the α,α,α,α-isomer of H_2TAPP was obtained in 65% yield using the atropisomerization methodology of Lindsey.[10] The urea appended porphyrins **2**−**5** (Figure 1) were synthesized by the addition of 4 equiv of the requisite aromatic isocyanate to the α,α,α,α-atropisomer of H_2TAPP in chloroform at room temperature and were obtained as purple microcrystalline solids in yields ranging from 70 to 85% after purification by silica gel column chromatography and subsequent recrystallization from CH_2Cl_2/hexane. The model tetraphenylporphyrin (TPP) was prepared using standard literature procedure.[11]

^{1}H NMR and UV/vis Characterization of Receptors. The ^{1}H NMR spectra of **2**−**5**, recorded in DMSO-d_6 at ambient temperature, revealed a broad singlet in the range −2.60 to −2.66 ppm due to the porphyrin NH protons resonance H_h (Figure 1), whereas the typical eight β-pyrrole protons (H_a) appeared as a singlet in the range 8.7−8.8 ppm. The singlet resonance of the β-pyrrole protons was indicative of the α,α,α,α conformation of the molecules. The resonances for the attached urea NH protons ($H_{f,g}$) and the porphyrin *meso*-phenyl ring protons (H_{b-e}) were generally found between 7.5 and 8.5 ppm. In all cases, the urea NH protons were observed as two broad singlets, with one resonating more than 0.5 ppm downfield from the other. The proton resonance farthest downfield is presumably the set of (mostly H_g) protons, which the X-ray crystal analysis (vide infra) showed was H-bonded to three DMSO molecules. The proton resonances of zinc complexes **6**−**8**, in comparison to the free-base ligands, were noted at higher field, and the α,α,α,α conformation of the molecule was retained.

The UV/vis spectra of porphyrins **2**−**5** revealed porphyrinoid features with intense Soret and four *phyllo* type (IV > II > III > I) Q-bands in the range 421−424 nm and 518−650 nm, respectively. In comparison to TPP, the Soret (B) and Q-bands for these new ligands were red shifted. As with ^{1}H NMR, the optical absorption data for the zinc complexes strongly suggest that there was no gross change in macrocyclic structure upon metalation. Only the disappearance of the Q-bands (III and IV) and the appearance of the α and β bands were observed for these complexes, consistent with the optical absorption spectroscopy observed for other metalated zinc porphyrins.[12] The proposed structures **2**−**8** were corroborated by high-resolution FAB-mass spectrometry, elemental analysis, and X-ray crystallography (see the Experimental Section).

Anion Coordination Studies. Quantification of the association constants of neutral hosts **2**−**5**, **6**, and **8** was accomplished

(6) Jagessar, R. C.; Burns, D. H. *J. Chem. Soc., Chem. Commun.* **1997**, 1685−1686.
(7) Král, V.; Furuta, H.; Shreder, K.; Lynch, V.; Sessler, J. L. *J. Am. Chem. Soc.* **1996**, *118*, 1595−1607.
(8) (a) Beer, P. D.; Drew, M. G. B.; Hesek, D.; Jagessar, R. *J. Chem. Soc., Chem. Commun.* **1995**, 1187. (b) Beer, P. D.; Drew, M. G. B.; Jagessar, R. *J. Chem. Soc., Dalton Trans.* **1997**, 881.
(9) Collman, J. P.; Gagne, R. R.; Reed, C. A.; Halbert, T. R.; Lang, G.; Robinson, W. T. *J. Am. Chem. Soc.* **1975**, *97*, 1429.
(10) Lindsey, J. S. *J. Org. Chem.* **1980**, *45*, 5215.
(11) Adler, A. D.; Longo, F. R.; Finarelli, J. D.; Goldmacher, J.; Assour, J.; Korsakoff, L. *J. Org. Chem.* **1967**, *32*, 476.
(12) Maillard, P.; Guerqurn, K.; Huel, J. L.; Momenteau, M. *J. Org. Chem.* **1993**, *58*, 2774.

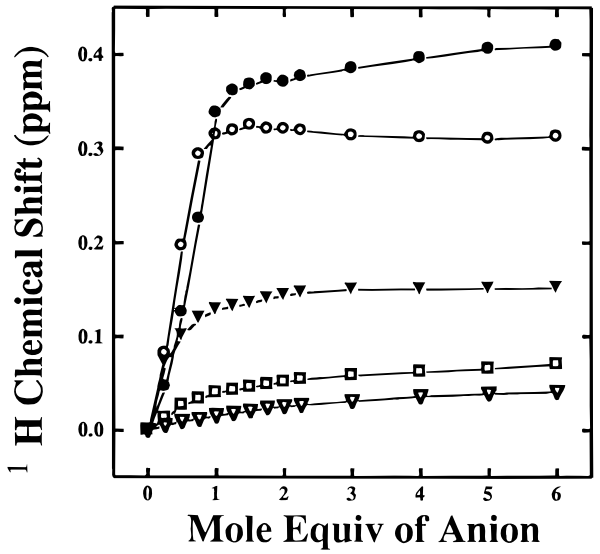

Figure 2. Titration curves of porphyrin **4** plus anions: ● = $H_2PO_4^-$, ○ = Cl^-, ▼ = Br^-, □ = HSO_4^-, and ∇ = NO_3^- (tetrabutylammonium counterion).

by following the titrations of the anions with ^{1}H NMR spectroscopy in the strongly solvating solvent DMSO-d_6 and, where necessary, in the more highly competitive mixed solvent system DMSO-d_6/D_2O (88:12, v/v). The anions Cl^-, Br^-, NO_3^-, HSO_4^-, and $H_2PO_4^-$ were added as their tetrabutylammonium salts. Examples of titration binding curves with porphyrin **4** and representative anions are shown in Figure 2. The association constants were determined by nonlinear regression analysis using the computer program EQNMR.[13]

In all cases, shifts were observed for the receptor porphyrin *meso*-phenyl, β-pyrroles, porphyrin NH, urea NH, and urea phenyl protons. Three sets of protons exhibited invariant shifts upon complexation: the β-pyrrole protons always shifted upfield, the urea NH protons always moved downfield, and the porphyrin NH always moved downfield. Significant shifts were observed for the urea NH protons, with the farthest downfield of the two urea NH resonances the most perturbed. For example, downfield shifts of 0.5 ppm were observed after the addition of 1 equiv of chloride, and downfield shifts of 1 ppm were observed after the addition of 2−3 equiv of dihydrogen phosphate anion. The large shift of the urea NH protons was indicative of their essential role in the anion recognition process via hydrogen bonding.[3e−f,14] The fact that the β-pyrrolic protons remained a sharp singlet upon anion complexation suggested that the anion was bound in the urea pocket of the porphyrin. The consistent upfield shift of the β-pyrrole protons coupled with the downfield shift of the porphyrin inner imino protons upon anion complexation indicated that the anion was affecting (decreasing) the porphyrin ring current. Thus, the porphyrin macrocycle was both a scaffold for the urea functional groups and concomitantly a sensor for the anion's electrostatic field.

The association constants for **2**−**5**, **6**, and **8** with various anions in DMSO-d_6 are presented in Table 1. For all free-base porphyrins, the binding of Cl^- was calculated to be greater than 10^5 M^{-1} in DMSO-d_6 (indicative of an extremely stable receptor complex formation), so it was impossible to judge any selectivity in binding that might be occurring for this anion between the differently para-substituted porphyrins **2**−**5** in this solvent.[15] These association constants are far larger than those that have been previously reported for urea- and nonurea-functionalized anion receptors that bind chloride.[1,7,9,14,16] To ascertain if the para substituents modulated the porphyrins ability to bind chloride anion, a more competitive solvent system was sought. Titration of the porphyrin receptors in a 12% D_2O/DMSO-d_6 solvent mixture with TBACl resulted in a decrease in the respective association constants by a factor of approximately 10^2. This placed the binding constants in a range that allowed selectivity trends with the various porphyrins to be determined and for a comparison to those already determined for the other anions with titration in DMSO-d_6.

Table 1. Association Constants for Porphyrins **2**−**5**, **6**, and **8** and Cl^-, Br^-, NO_3^-, HSO_4^-, and $H_2PO_4^-$ Anions in DMSO-d_6 and DMSO-d_6/D_2O (88:12)[a]

porphyrin	K (M^{-1}) Cl^-	K (M^{-1}) Br^-	K (M^{-1}) HSO_4^-	K (M^{-1}) NO_3^-	K (M^{-1}) $H_2PO_4^-$
2	$>1 \times 10^5$ 1.36×10^3 [b]	1.01×10^4	115	90	400
3	$>1 \times 10^5$ 1.02×10^3 [b]	1.004×10^4	137	60	300
4	$>1 \times 10^5$ 9.73×10^3 [b]	9.99×10^3	147	55	1.4×10^3
5	$>1 \times 10^5$ *c*	1.005×10^4	226	163	9.56×10^3
6	9.5×10^3	1.51×10^3	*d*	23	49
8	9.82×10^3	1.1×10^3	*d*	*d*	489

[a] Association constants determined from nonlinear regression analysis using the program EQNMR, with errors ranging from ±10 to 20%. [b] Association constants determined in DMSO-d_6/D_2O 88:12, v/v. [c] No association constant was determined due to precipitation in DMSO-d_6/D_2O 88:12, v/v. [d] Broadness in porphyrin proton resonances made it impossible to determine association constant accurately.

The modification of the urea phenyl ring with electron-withdrawing para substituents was anticipated to increase the acidity of the urea NH's and in turn increase the strength of the hydrogen bonds formed between the urea NH's and the anions.[3a,14a] Porphyrin **5**, with a para-substituted nitro group, did exhibit larger binding constants for the anions, and at the same time the selectivity trends ($Cl^- > Br^- > H_2PO_4^2 > HSO_4^-$, NO_3^-) were the same as for the rest of the receptors. Variations in binding constants (between 2- to 10-fold differences) were noted for the halides, nitrate, or bisulfate anions between the different porphyrin receptors. As shown in Table 1, the anion whose binding selectivity changed most significantly with the different porphyrin receptors was dihydrogen phosphate. The binding constants increased by a factor of 24 (from 400 for **2** to 9600 for **5**) as the electron-withdrawing power of the para substituent was increased. We first hypothesized that the large difference in selectivities observed for porphyrin receptors **2**−**5** toward phosphate was due to the anion's ability to act as a hydrogen-bond donor as well as acceptor. However, semiempirical calculations showed a trend of decreasing negative surface electrostatic potentials around the carbonyl and aromatic ring when phenylurea was elaborated with electron-withdrawing para substituents, a model inconsistent with the above speculation. The binding constant of the tetrahedral bisulfate anion was smaller than that of the tetrahedral dihydrogen phosphate anion, and this selectivity may be due primarily to the greater basicity of the dihydrogen phosphate anion, allowing it to form stronger hydrogen bonds with the urea NHs. This same property

(13) Hynes, M. J. *J. Chem. Soc., Dalton Trans.* **1993**, 311.

(14) (a) Hughes, M. P.; Smith, B. D. *J. Org. Chem.* **1997**, *62*, 4492−4499. (b) Hamann, B. C.; Branda, N. R.; Rebek, J. *Tetrahedron Lett.* **1993**, *34*, 6837. (c) Fan, E.; van Arman, S. A.; Kincaid, S.; Hamilton, A. D. *J. Am. Chem. Soc.* **1993**, *115*, 369.

(15) Binding constants greater than 10^5 M^{-1} cannot be determined accurately: Wang, T.; Bradshaw, J. S.; Izatt, R. M. *J. Heterocycl. Chem.* **1994**, *31*, 1097.

may also be responsible for the greatest differences seen in binding constants with this anion and the different porphyrin receptors.

The binding for bromide was high ($K_a = 1.0 \times 10^4$) but was smaller than that of chloride. The overall strong binding of bromide anion among the different porphyrins, however, corroborated the selectivity these receptors exhibit for anions that are spherical. The difference in binding selectivity between the chloride and bromide anions may partially result from the stronger hydrogen-bonding accepting properties of the chloride anion, since it has a higher charge density than the larger bromide anion. The selectivity trend $Cl^- > Br^- > H_2PO_4^-$ displayed by these receptors is novel for any urea anion-binding system, except for Reinhoudt's calixarenes, where the pocket is too small for the phosphate anion to ever fit.[3f] Analysis of the X-ray crystal data (vide infra) suggests that an ordered solvent molecule, hydrogen bonded to the host in the porphyrin pocket, also plays an important role in anion discrimination. The four urea groups of receptors **2**−**5** bounded by the porphyrin plane creates a pocket that, with the inclusion of complexed solvent, delineates a cavity optimized for the binding of a negatively charged spheroidal shape.

The anion coordination studies of the zinc(II) complexes of **6** and **8** showed that the porphyrins exhibited a loss both in selectivity and binding strength, compared to their parent free-base porphyrins. It was anticipated that the metal might act as an additional anion-binding site orthogonal to the urea hydrogens and, thereby, increase the overall binding interaction (as observed with other multisite porphyrins, such as Beer's ferrocene porphyrin, that only binds anions when metalated[8b]). The zinc(II) complexes, while exhibiting the same general selectivity trend of $Cl^- > Br^- > H_2PO_4^{2-}$, NO_3^-, exhibited a chloride−nitrate and chloride−dihydrogen phosphate selectivity that was lowered compared to the corresponding free-base urea porphyrins (Table 1). The binding constants for chloride, bromide, and dihydrogen phosphate were three to 10 times less than with their respective free-base porphyrin receptors. This decrease in selectivity and binding strength for the zinc(II) complexes may be attributable to an increase in rigidity of the metalloporphyrin over that of the free-base receptor. This rigidity, in turn, would affect the flexibility and positioning of the urea groups required for optimal hydrogen bonding, as exemplified by the free-base urea analogues. On the other hand, zinc(II) porphyrins can be pentacoordinate, and thus, coordination to the metal could occur on the side of the porphyrin opposite to the urea pocket (bottom-bound). Anion coordination to the metal opposite the urea pocket would be expected to show no change in the ^{1}H NMR spectrum in the same way that ZnTTP exhibits no real change in its ^{1}H NMR spectrum upon anion coordination. If this type of "nonspecific" binding were extensive, it would reduce the apparent binding constant because it would reduce the effective concentration of free anion. However, the binding of bromide and chloride anions to ZnTTP in dichloromethane has been determined to be relatively weak, with $K = 15$ and 300, respectively.[17] Assuming a bottom-bound anion species had a similar binding constant, its concentration would be insignificant compared to the species where the anion was bound in the porphyrin urea pocket (i.e., with a ratio of binding constants of approximately 10^3:1). Additionally, the X-ray crystal structure of metalloporphyrin **7** shows DMSO bound to the metal on the underside of the porphyrin pocket (vide infra), demonstrating that in DMSO the solvent would effectively compete with this kind of anion-bonding motif. Certainly the fact that anion binding induces significant shifts of all the respective host protons suggests that anion coordination in solution is occurring mainly in the urea-binding pocket of these metalloporphyrins.

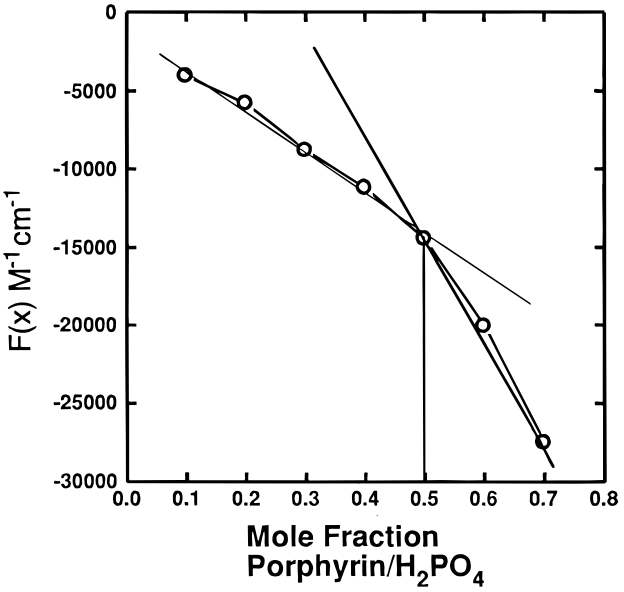

Figure 3. Job plot of porphyrin **4** + $H_2PO_4^-$ (tetrabutylammonium counterion).

Anion binding to the free-base porphyrins was also characterized qualitatively with UV/vis spectroscopy. UV/vis spectral anion titration revealed anion binding through perturbation of the Soret and visible Q-bands of **2**−**4**, when Cl^-, Br^-, HSO_4^-, $H_2PO_4^-$, and NO_3^- anions were added as their tetrabutylammonium salts. Porphyrins **2**−**5** were first placed in a 0.1 M solution of $TBAPF_6$, and when titrated with the usual anions, their Soret bands would exhibit a red shift with a concomitant increase in intensity (the added $TBAPF_6$ produced an environment of constant ionic strength, and the PF_6 anion did not bind to the porphyrin receptors due to its large size). Changes in the Soret band upon titration with the anions suggest that the anions were bound within the porphyrin−urea pocket. Under analogous titration conditions, the model compound, tetraphenylporphyrin, exhibited negligible perturbation in its ^{1}H NMR and UV/vis spectra, indicating that the changes observed with ligands **2**−**8** were truly indicative of anion binding.

The very strong binding of Cl^- ion allowed the mole ratio method[18] to be used in the determination of the binding stoichiometry, which was found to be 1:1 for all four porphyrins. Job's method of continuous variation[18] was used to determine the stoichiometry of binding with bromine, dihydrogen phosphate, hydrogen sulfate, and nitrate anions for receptor **4**. Figure 3 illustrates the Job plot of dihydrogen phosphate anion, determined by utilizing the method of Tran-Thi and Lipskier[19] (UV/vis spectrophotometry, 0.1 M $TBAPF_6$). All Job plots conformed to a 1:1 binding stoichiometry illustrated by the inflection point at a mole fraction of 0.5. Fluoride anion, on the other hand, had completely different binding characteristics from all the above anions, exhibiting apparent allosteric binding

(16) (a) Kavallieratos, K.; de Gala, S. R.; Austin, D. J.; Crabtree, R. H. *J. Am. Chem. Soc.* **1997**, *119*, 2325. (b) Davis, A. P.; Perry, J. J.; Williams, R. P. *J. Am. Chem. Soc.* **1997**, *119*, 1793. (c) Berger, M.; Schmidtchen, F. P. *J. Am. Chem. Soc.* **1996**, *118*, 8947. (d) Gale, P. A.; Sessler, J. L.; Král, V.; Lynch, V. *J. Am. Chem. Soc.* **1996**, *118*, 5140.

(17) Nappa, M.; Valentine, J. S. *J. Am. Chem. Soc.* **1978**, *100*, 5075−5080.

(18) Connors, K. A. *Binding Constants*; John Wiley & Sons: New York, 1987; pp 24−28.

(19) Lipskier, J. F.; Tran-Thi, T. H. *Inorg. Chem.* **1993**, *32*, 722−731.

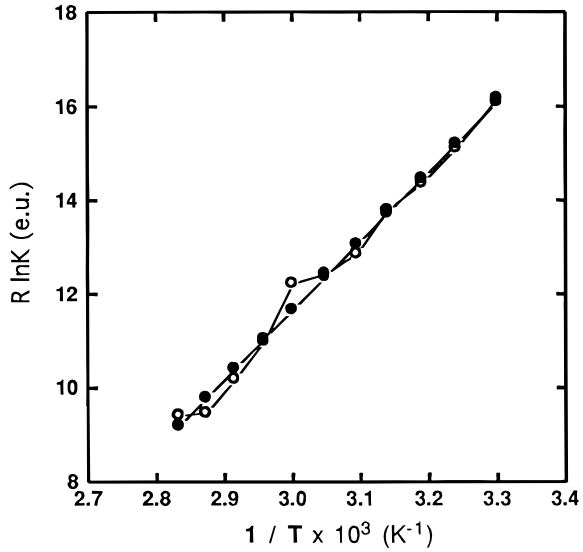

Figure 4. van't Hoff plot of porphyrin **4** + TBABr: ○ = data, ● = linear least-squares fit from which thermodynamic data was determined.

effects with a 2:1 complexation stoichiometry (to be presented elsewhere[20]).

A variable-temperature ^{1}H NMR experiment utilizing the method of Dougherty et al.[21] was undertaken to examine the thermodynamic parameters involved in anion binding. Upon an increase in temperature, shifts in the proton resonances of the porphyrin showed that the binding constant was diminishing, i.e., that the pocket was becoming less amenable to tight complexation. The van't Hoff plot of the 1:1 complex of porphyrin **4** and TBABr, shown in Figure 4, was used to determine the enthalpy and entropy of complexation.. The ΔH of the complexation was quite favorable and the ΔS of complexation unfavorable, with values of $\Delta H = -14.8$ kcal/mol and $\Delta S = -32.7$ eu. Similar thermodynamic parameters have been observed with Beer's neutral ferrocene anion receptor.[22] Here, the large enthalpy of complexation associated with a large decrease in the entropy of complexation is presumably due to the formation of several hydrogen bonds to the anion via the urea functional groups and, possibly, a (highly ordered) solvent molecule assisted interaction (vide infra) as well, resulting in a large association constant.

X-ray Crystal Structures. Crystals of free-base **3** complexed with bromide and chloride anion, as well as uncomplexed metalloporphyrin **7**, suitable for X-ray crystallographic analysis were grown by slow evaporation from DMSO. The ORTEP diagram of the metalloporphyrin **7** (viewed from the top) is detailed in Figure 5 with additional views (Figures S1 and S2) in the Supporting Information. The crystal data and refinement results of **7**·5DMSO, **3** + TBABr·5DMSO, a related solvate **3** + TBABr·3DMSO, and **3** + TBACl·5DMSO are presented in Table 2. The crystal structure of **7**·5DMSO shows that three of the urea groups have their NH pointed toward the inside of the porphyrin macrocycle, and their urea carbonyls are pointed toward the outside of the ring, while one urea has its carbonyl and NH more or less orthogonal to the macrocyclic ring, and there is no self-association of the urea groups. The ureas are bound to three DMSO molecules, two of which are located between the pickets on the periphery of the porphyrin and one

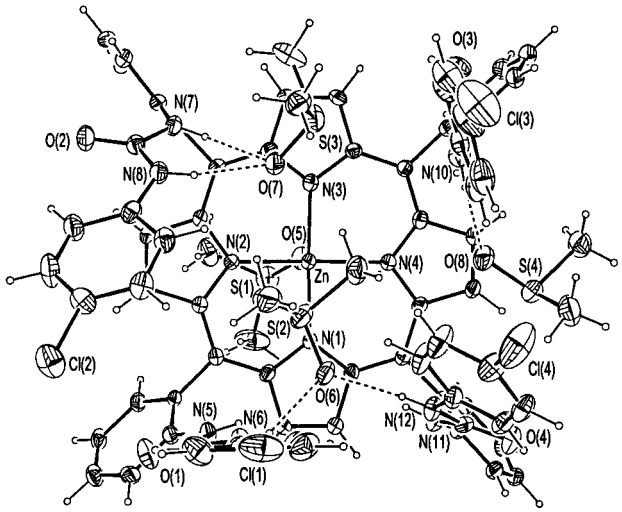

Figure 5. ORTEP diagram illustrating the molecular structure of porphyrin **7**·5DMSO. The porphyrin plane is in the plane of the paper, and the O-coordinated axial DMSO ligand is below the plane. Selected atoms in the drawing are labeled with the atom names given in the tables. 50% probability ellipsoids are displayed.

that is more centered in the pocket. The former two DMSO solvent molecules are each bound to one urea via two hydrogen bonds, while the latter DMSO solvent molecule is hydrogen bonded to two ureas via two hydrogen bonds. This corroborates what was seen in the ^{1}H NMR in DMSO-d_6, where the urea hydrogens were found very far downfield due to hydrogen bonding with the solvent. In **7**, the coordinated DMSO and the zinc metal ion are found on the side of the porphyrin plane opposite the urea pickets. This is in distinct contrast to most picket fence porphyrin derivatives where the ligand and metal are found in the pocket. Clearly, the hydrogen-bonded DMSO molecules provide substantial stabilization of extended urea pickets.

The ORTEP diagrams of porphyrin **3** (viewed from the top), complexed to both bromide and chloride anion (**3** + TBABr·5DMSO and **3** + TBACl·5DMSO), are detailed in Figures 6 and 7, respectively. Additional views of these two molecules are given in Figures S3 and S4 of the Supporting Information. Also presented in the Supporting Information are Figures S5 and S6, which display equivalent information for the related solvate **3** + TBABr·3DMSO. The disposition of the urea functional groups about the porphyrin ring is the same as that of the metalated species **7**. The ORTEP diagrams show the anion deeply buried in the pocket of the porphyrin receptor, positioned over one pyrrole. The crystal structures corroborate the Job plot 1:1 stoichiometric analysis; presumably, the buildup of more than one negative charge within the neutral porphyrin receptor is thermodynamically unfavorable. On opposite sides of the anion are two adjacent ureas that are hydrogen bonded via the four NH protons, with NH−Br distances between 2.4 and 2.8 Å and NH−Cl distances between 2.3 and 2.7 Å. A TBA cation lies outside the pocket, and in the case of the **3** + TBABr·5DMSO and **3** + TBACl·5DMSO complexes, a DMSO molecule is positioned in the center of the pocket. The electron-deficient sulfur is in near van der Waals contact with the chloride or bromide anion, suggesting a Coulombic interaction. The **3** + TBABr·3DMSO complex shows a DMSO molecule slightly off-center of the pocket that is positioned such that one of its methyl groups is close to the anion, precluding a Coulombic interaction beetween the sulfur and anion.

The X-ray structures in all three characterized species clearly show that the complexation of the halide anions occurs via four

(20) Jagessar, R. C.; Burns, D. H.; Scheidt, W. R. Unpublished data.
(21) Stauffer, D. A.; Barrans, R. E.; Dougherty, D. A. *J. Org. Chem.* **1990**, *55*, 2762−2767.
(22) Beer, P. D.; Graydon, A. R.; Johnson, O. M.; Smith, D. K. *Inorg. Chem.* **1997**, *36*, 2112−2118.

Table 2. Crystal Data and Refinement Results

complex	**7**·5DMSO	**3** + TBABr·3DMSO	**3** + TBABr·5DMSO	**3** + TBACl·5DMSO
		$C_{91.32}H_{97.98}Br_{0.83}$	$C_{94.11}H_{107.25}Br_{0.75}$	
empirical form	$C_{82}H_{78}Cl_4N_{12}O_9S_5Zn$	$Cl_4N_{12.83}O_7S_3$	$Cl_4N_{12.76}O_9S_5$	$C_{98}H_{116}C_{l5}N_{13}O_9S_5$
fw, amu	1743.03	1792.10	1923.50	1957.59
space group	$P\bar{1}$	$P\bar{1}$	$P\bar{1}$	$P\bar{1}$
T, K	130	130	130	130
a, Å	13.442(3)	15.349(2)	14.677(3)	14.662(1)
b, Å	14.688(2)	17.651(2)	15.853(2)	15.846(1)
c, Å	21.738(7)	18.949(2)	22.542(2)	22.527(3)
α, deg	88.54(1)	93.92(2)	98.41(1)	98.41(2)
β, deg	80.78(1)	96.97(1)	93.93(1)	93.77(1)
λ, deg	77.72(1)	115.66(1)	106.60(1)	107.03(1)
V, Å^3	4139	4551.4	4938.6	4917.9
Z	2	2	2	2
final *R* indices, [$I > 2\sigma(I)$]	$R_1 = 0.0823$, $wR_2 = 0.1572$	$R_1 = 0.0768$, $wR_2 = 0.1759$	$R_1 = 0.0936$, $wR_2 = 0.2276$	$R_1 = 0.0821$, $wR_2 = 0.1903$
R indices (all data)	$R_1 = 0.1524$, $wR_2 = 0.1955$	$R_1 = 0.1418$, $wR_2 = 0.2180$	$R_1 = 0.1679$, $wR_2 = 0.2841$	$R_1 = 0.1361$, $wR_2 = 0.2298$
goodness-of-fit on F^2	1.031	1.016	1.014	1.019

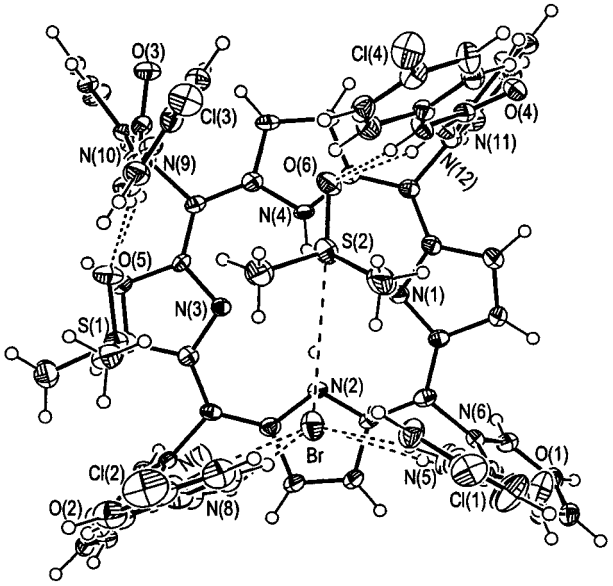

Figure 6. ORTEP diagram illustrating the geometry of the bound Br^- in the system **3** + TBABr·5DMSO. The position of the two DMSO molecules in the binding pocket are clear. The porphyrin plane is in the plane of the paper. 50% probability ellipsoids are displayed. The location of the two inner hydrogen atoms of the free base are also shown.

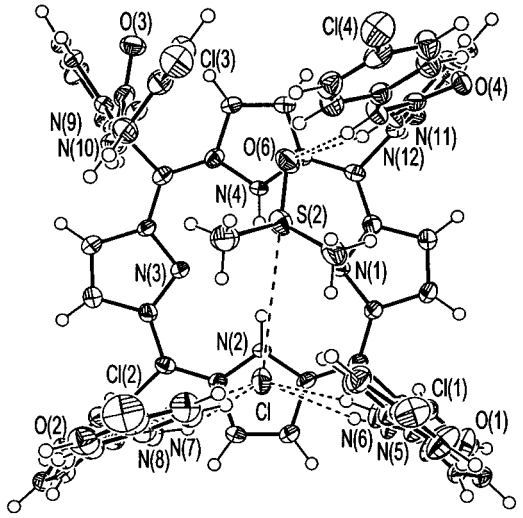

Figure 7. ORTEP diagram illustrating the geometry of the bound Cl^- in the system **3** + TBACl·5DMSO showing the same information as given in Figure 6.

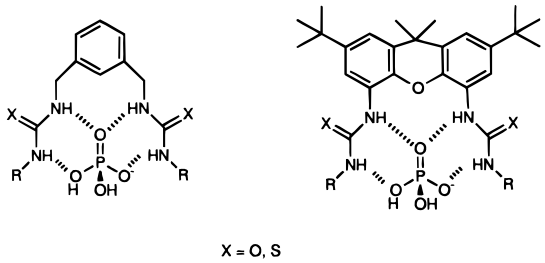

Figure 8. Bühlmann urea receptors bound to dihydrogen phosphate anion.

hydrogen bonds that originate from two adjacent urea functional groups. The question can be raised as to why is the selectivity of this system reversed from other bis-urea systems, where phosphate is found to be stronger binding than chloride.[3a,d] Indeed, to our knowledge, the only urea receptors reported to date that exhibit selectivity for halides are Reinhoudt's calixarene−urea receptors,[3e,f,h] where phosphate anion is not competitive because it is too large to bind within the urea cavity. As an example, the phenyl and xanthene bis-ureas (Figure 8) of Bühlmann et al.[3a,d] bind dihydrogen phosphate anion stronger than halide anions in DMSO, results opposite to those found with our receptor. CPK model analysis and analysis of the porphyrin crystal structures show that the two receptors exhibit only small differences in the spacing between the urea functional groups. It is to be noted that, unlike Bühlmann's bis-ureas, the urea functional groups that sit over the porphyrin ring cannot be accessed by the anion from below. However, the difference in structures are not so dramatic that one would anticipate this reversal of binding affinities. Indeed, the CPK analysis certainly shows that phosphate should be able to hydrogen bond with the two ureas via four hydrogen-bonding interactions (as is postulated for Bühlmann's receptors, Figure 8) *unless there is solvent in the porphyrin pocket*. Dihydrogen phosphate anion, allowed to hydrogen bond in just such a fashion in the porphyrin pocket, would necessitate the removal of an ordered (i.e., hydrogen bonded with a urea) solvent molecule of DMSO, where the binding of chloride or bromide anion does not. Consequently, to attain the same effective bonding interactions (four hydrogen bonds) as the halides, the binding of the larger, tetrahedral phosphate anion would require an additional expense in energy due to the desolvation of DMSO from the porphyrin pocket. This kind of solvent effect would be as likely a contributor to the overall high affinity the porphyrin receptors

exhibit for halide anions as is the shape of the pocket. While a solid-state structure may not portray the solution-state structure exactly, there are likely as many, if not more, solvent molecules associated with the porphyrin in solution then in the crystal structure; the crystal structure showed the porphyrin receptor to be highly solvated (vide supra). Therefore, it is likely that in solution a DMSO molecule is hydrogen bonded to a urea so as to position it in the porphyrin cavity as seen in the crystal structure. With the porphyrin−TBACl complex, the ordered position of the pocket DMSO allows it to solvate the chloride anion; i.e., the chloride anion and porphyrin receptor do not need to be fully desolvated for binding to occur. This kind of favorable solvation effect for the complexation of chloride anion is similar to the favorable solvation effects discussed by Nolte,[23] Collet,[24] and Still[25] to explain the observed increase in binding constants of host−guest complexes when desolvation of the host was unnecessary. It is also reminiscent of the effect, witnessed by Bonnar-Law and Sanders,[26] that an ordered, bound solvent molecule has on the increase in sugar binding strength of a steroid-capped porphyrin. Thus, complexation with four hydrogen bonds and concomitant continued solvation by DMSO (both the porphyrin−host and anion−guest) would explain why chloride anion is so tightly bound to the porphyrin receptors **2**−**5**. Certainly, this type of bonding motif would explain the rather large favorable enthalpy of complexation and unfavorable entropy of complexation determined from the variable-temperature ^{1}H NMR experiment. Unfortunately, we were unable to determine solvent effects, if any, on binding by switching to other solvents. The use of acetone-d_6 in place of DMSO gave rise to very large binding constants and the same anion selectivities. Solubility constraints precluded the use of CD_3OD and the non-hydrogen-bonding solvents CD_3Cl or CD_2Cl_2. Titration experiments with TBABr and porphyrins **2** and **3** in 88% DMSO-d_6/12% D_2O showed that the receptors, in this solvent system, expressed only a slightly higher affinity for chloride over bromide anion.

Conclusions

The first neutral porphyrin anion receptors **2**−**5**, with picket urea functional groups, have been prepared and found to bind anions with the unique selectivity of $Cl^- > Br^- \gg H_2PO_4^- > HSO_4^- > NO_3^-$ in DMSO. The K (M^{-1}) of complexation for Cl^- was greater than 10^5, and the receptors all exhibited a Cl^- binding selectivity of greater than 10:1 with Br^-, greater than 280:1 with $H_2PO_4^-$, and greater than 1000:1 with NO_3^- and HSO_4^-. Even in the more competitive solvent system of 88% DMSO-d_6/12% D_2O, the porphyrins **2**−**4** bound the chloride anion with a K (M^{-1}) $\approx 10^3$. The porphyrin receptors **2**−**5**, **6**, and **8** showed similar binding constants for any one anion, except for dihydrogen phosphate, where the K (M^{-1}) increased concomitantly with an increase in the urea−phenyl parasubstituent electron-withdrawing capability. Mole ratio and Job analysis of anion binding showed the stoichiometry of the anions complexation with porphyrin **4** to all be 1:1, which was corroborated by crystal structures of the TBACl and TBABr complexes of porphyrin **3**. A van't Hoff analysis of the porphyrin **4**−TBABr complex determined the enthalpy of binding to be very favorable and the entropy of complexation to be unfavorable ($\Delta H = -14.8$ kcal/mol and $\Delta S = -32.7$ eu). The X-ray crystal structure of uncomplexed **7** showed the metalloporphyrin to be highly solvated, with three DMSO molecules hydrogen bonded to the urea functional groups. The X-ray crystal structures of **3** complexed with TBABr and TBACl showed that the halide was buried deep within the urea pickets and bound to adjacent urea functional groups via four hydrogen bonds. In all crystal structures, a DMSO molecule was found in the porphyrin pocket, bound to a urea via two hydrogen bonds. The DMSO precluded dihydrogen phosphate from the formation of four hydrogen bonds between two adjacent ureas without the added expense of desolvation of the porphyrin pocket. On the other hand, the spherical halides form four hydrogen bonds while the porphyrin still remains highly solvated. Additionally, in the case of the **3** + TBABr·5DMSO and **3** + TBACl·5DMSO complexes, the DMSO was positioned in such a way as to allow an attractive Coulombic interaction between the anion and the electron-poor sulfur. Thus, the orientation and nature of the functional groups that make up the pickets on the porphyrin (i.e., two ureas that bind the anion and the other two that bind and order solvent) are most complementary with the spherical halide anions. Further studies which examine the role that competitive solvents play in the selectivity of anion recognition are in progress.

Experimental Section

Materials and General Procedures. Reagent-grade benzene, chloroform, and dichloromethane were obtained from Fisher and used without further purification: methanol was distilled from Mg and stored over 3 Å molecular sieves. Pyrrole and 2-nitrobenzaldehyde were obtained from Aldrich. All melting points (Mel-Temp) are uncorrected. ^{1}H NMR spectra were recorded at 300 MHz in DMSO-d_6 with Me_4Si as an internal standard unless otherwise specified. Silica gel (Davisil 633) was used for column chromatography, and analytical thin-layer chromatography (TLC) was performed using precoated Whatman PE SIL G/UV. UV/vis spectroscopy were carried out on a Shimadzu model 1600 UV/vis spectrophotometer. FAB mass spectra were obtained on a VG ZAB high-resolution mass spectrometer by Dr. Todd Williams at the University of Kansas. Elemental analysis was done by Desert Analytics, Tucson, AZ.

Binding Studies. Titration of a 0.5 mL (5 mM, where no self-association is observed) solution of the porphyrin receptor in an NMR tube with stepwise addition of 0−6 equiv of the anions as their tetrabutylammonium salts was followed by ^{1}H NMR spectroscopy, and the spectrum was recorded after each addition. Changes in the urea NH, *β*-pyrrole, *meso*-phenyl, and porphyrin NH protons were monitored. Titration curves were generated by plotting the respective changes in chemical shifts versus the molar equivalents of anion. The association constants were determined by nonlinear regression analysis of these curves using the computer program EQNMR and fitting the data to a 1:1 binding stoichiometric model (determined from molar ratio plots and Job plot analysis, see below). Qualitative UV/vis anion-binding studies were carried out by first recording the spectra of the free ligand, followed by adding the required stoichiometric amounts of the anion and recording changes in the UV/vis spectrum.

Structure Determinations. Structural analyses for crystals of **7**, **3** + TBABr-3DMSO, **3** + TBABr-**5**DMSO, and **3** + TBACl-5DMSO were carried out on an Enraf-Nonius FAST area detector diffractometer at 130 K by methods and procedures described previously.[27] A brief summary of crystal data and data collection parameters is given in Table

(23) Reek, J. N. H.; Priem, A. H.; Engelkamp, H.; Rowan, A. E.; Elemans, J. A. A. W.; Nolte, R. J. M. *J. Am. Chem. Soc.* **1997**, *119*, 9956−9964.

(24) Canceill, J.; Lacombe, L.; Collet, A. *J. Am. Chem. Soc.* **1986**, *108*, 4230.

(25) Chapman, K. T.; Still, W. C. *J. Am. Chem. Soc.* **1989**, *111*, 3075.

(26) Bonar-Law, R. P.; Sanders, J. K. M. *J. Am. Chem. Soc.* **1995**, *117*, 259.

(27) Scheidt, W. E.; Turowska-Tyrk, I. *Inorg. Chem.* **1994**, *33*, 1314.

(28) Programs used in this study included SHELXS-86 (Sheldrick, G. M. *Acta Crystallogr., Sect. A* **1990**, *A46*, 467), SHELXL-93 (Sheldrick. G. M. *J. Appl. Crystallogr.*, manuscript in preparation), and local modifications of Johnson's ORTEP2. Scattering factors were taken from *International Tables for Crystallography*; Wilson, A. J. C., Ed.; Kluwer Academic Publishers: Dordrecht, 1992; Vol. C.

2. All structures were solved by direct methods with SHELXS-86.[28] All structures were refined against F^2 with the SHELXL-94 program.[28] Nearly all hydrogen atoms were located in difference Fourier syntheses. In the final refinements, the hydrogen atoms were treated as idealized riding atoms (C−H = 0.95 Å for R_2CH, 0.98 Å for RCH_3). In some structures, bond length restraints were applied to the solvent molecules and urea N−H bonds by the use of free variables. In **7**, one DMSO solvent molecule was found to be disordered in a way that the sulfur and oxygen atoms were located on two sets of positions. For **3** + TBABr-3DMSO, one butyl group of the tetrabutylammonium cation was found to be disordered so that two carbon atom were located on two sets of positions. In **3** + TBABr-5DMSO and **3** + TBACl-5DMSO, which were found to be isomorphous, two DMSO solvent molecules were found to be disordered such that the sulfur atom was located on both sides of a plane defined by the oxygen and the two methyl carbon atoms. Finally, in the crystals of the two bromide complexes, the apparent occupancy of the bromide ion was found to be less than full occupancy. This was treated as a variable in the least-squares refinements, and the occupancy of the TBA counterion was constrained to remain equal to that of bromide anion. We believe that the reduced occupancy of Br^- resulted from the exposure of the crystallizing solution to ambient humidity. All data sets were corrected for the effects of absorption using the programs DIFABS.[29] Final atomic coordinates for all four structures are available as Supporting Information.

Job Plots. Job plots were determined by UV/vis spectroscopy using a method adapted from Tran-Thi and Lipskier.[19] A stock solution of 0.1 M $TBAPF_6$ in dichloromethane was prepared along with separate solutions of the porphyrin and anion of a known molarity in 0.1 M $TBAPF_6$ in dichloromethane. The appropriate molar ratio of porphyrin and anion was added to a sample tube and the solution made up to a constant volume with the stock solution of 0.1 M $TBAPF_6$. UV/vis spectra were recorded at the 10 different molar concentrations of porphyrin and anion, while the total concentration of porphyrin and anion remained the same throughout. The absorption maxima of the Soret and Q-bands measured at a given wavelength for mixtures with various ratios of porphyrin and anion were used in the expression:

$$F(x) = \mathrm{d}(x) + x\epsilon_\mathrm{p} - \epsilon_\mathrm{p}$$

where x is the mole fraction of anion, ϵ_p is the molar absorptivity of the porphyrin, and $\mathrm{d}(x)$ is the actual optical density of the solution divided by the total concentration of porphyrin. Thus, $F(x)$ represents the deviation from additivity of the absorption mixture due to complex formation. Job plots were obtained by plotting $F(x)$ as x was continuously varied.

General Procedure for the Preparation of Free Base and Metalated (α,α,α,α)-5,10,15,20−Tetrakis (2-(arylurea)phenyl)porphyrins. Compounds **2**−**5** were prepared and purified in an analogous fashion. To the α,α,α,α isomer of H_2TAPP (0.27 g, 0.4 mmol) in chloroform (25 mL) at room temperature was added 4 equiv of the requisite isocyanate (1.6 mmol) in a dropwise fashion via an addition funnel over a period of 1 h. The mixture was stirred at room temperature and the progress of the reaction monitored by TLC analyses. When the reaction was complete (usually after 24 h), the mixture was taken up in H_2O (25 mL) and the organic layer separated, washed with brine (24 mL), and dried over Na_2SO_4. Solvents were removed in vacuo, and the crude product was purified by silica gel column chromatography (CH_2Cl_2/ethyl acetate 8:1; with this solvent system the mobility of the porphyrins were phenyl **2** > chloro **3** > fluoro **4** > nitro **5**). Further purification was done by recrystallization from dichloromethane/hexane, producing purple microcrystalline solids in yields ranging from 70 to 85%.

The zinc(II) complexes were also prepared in an analogous fashion. Typically, the requisite free-base porphyrin (4.1×10^{-6} mol) was taken up in dichloromethane (10 mL) followed by the addition of a solution of zinc(II) acetate dihydrate (0.05 g, 0.23 mmol) dissolved in methanol (5 mL). The resulting solution was stirred under nitrogen for 24 h. Solvents were removed *in vacuo*, leaving a red residue. Water (10 mL) was added and the mixture stirred for 30 min, then filtered. The crude red solid was purified by silica gel column chromatography (CH_2Cl_2/ethyl acetate, 8:1 or 4:1) followed by recrystallization from CH_2Cl_2/hexane, leaving a red powder. Yields varied between 90 and 95%.

(α,α,α,α)-5,10,15,20-Tetrakis(2-(phenylurea)phenyl)porphyrin (2). Yield, 70%; mp 225−229 °C; UV/vis CH_2Cl_2 λ max (lnϵ): 424 (11.97), 518 (8.55), 550 (8.8), 584 (8.22), 650 (7.86); ^{1}H NMR δ - 1.5 (s, 2H), 6.66−6.69 (m, 12H), 6.88−6.89 (s, 8H), 7.38 (t, 4H, J = 7.23 Hz), 7.66 (br s, 4H), 7.73−7.80 (m, 8H), 8.36 (d, 4H, J = 8.79 Hz), 8.45 (br s, 4H), 8.76 (s, 8H); ^{13}C NMR δ 115.69, 117.58, 121.51, 121.62, 122.02, 128.42, 129.09, 131.22, 131.47, 135.36, 138.91, 139.13, 152.490; HRFAB MS *mz* calcd for $C_{72}H_{54}N_{12}O_4$ 1151.4469, found 1151.4446 (M + 1); Anal. Calcd for $C_{72}H_{54}N_{12}O_4$·$CHCl_3$: C, 69.00; H, 4.36; N, 13.22. Found: C, 69.35; H, 4.75; N, 12.86.

Zn(II) (α,α,α,α)-5,10,15,20-tetrakis(2-(phenylurea)phenyl)porphyrin (6). Yield, 95%; UV/vis: CH_2Cl_2 λ max (lnϵ): 426 (9.52), 562 (7.99), 513 (6.44); ^{1}H NMR δ 6.62 (m, 12H), 6.98 (d, 8H), 7.2 (br s, 4H), 7.41 (t, 4H, J = 9.24 Hz), 7.65−7.82 (m, 8H), 8.3 (br s 4H), 8.45 (d, 4H) 8.71 (s, 8H); HRFAB MS *mz* calcd for $C_{72}H_{52}N_{12}O_4Zn$ 1213.3604, found 1213.3557 (M + 1).

(α,α,α,α)-5,10,15,20-Tetrakis(2-(4-chlorophenylurea)phenyl)porphyrin (3). Yield, 76%; mp 220−224 °C; UV/vis: CH_2Cl_2 λ max (lnϵ): 424 (11.64), 517 (8.90), 592 (8.04), 650 (7.72); ^{1}H NMR δ − 2.66 (br s 2H), 6.95 (s, 16H), 7.42 (t, 4H; J = 7.1 Hz), 7.42 (t, 4H, J = 7.95 Hz;), 7.65 (br s 4H), 7.70−7.81 (m, 8H) 8.37 (d, 4H J = 8.4 Hz), 8.51 (br s, 4H), 8.78 (s, 8H); ^{13}C NMR δ 109.5, 115.54, 119.02, 121.64, 122.36, 125.08, 128.23, 129.12, 131.20, 131.47, 135.28, 138.13, 138.93, 152.39; HRFAB MS *mz* calcd for $C_{72}H_{50}N_{12}O_4Cl_4$ 1287.2910, found 1287.2876 (M + 1); Anal. Calcd for $C_{72}H_{50}N_{12}O_4Cl_4$·$CHCl_3$: C, 62.25; H, 3.64; N, 11.93. Found C, 63.04; H, 4.20; N, 11.90.

Zn(II) (α,α,α,α)-5,10,15,20-tetrakis(2-(4-chlorophenylurea)phenyl)porphyrin (7). Yield: 95%; mp 210 - 213 °C; UV/vis (CH_2Cl_2/benzonitrile) λ max (lnϵ): 428 (14.60), 475 (11.79), 556 (11.73); ^{1}H NMR δ 6.90 (s, 16H), 7.39 (t, 4H, J = 7.44 Hz), 7.56 (br s, 4H), 7.74−7.81 (m, 8H), 8.41 (d, 4H, J = 7.92 Hz), 8.66 (s, 8H), 8.92 (br s, 4H); HRFAB MS *mz* calcd for $C_{72}H_{48}N_{12}O_4Cl_4Zn$ 1349.2045, found 1349.2098 (M+1); Anal. Calcd for $C_{72}H_{48}N_{12}O_4Cl_4$.Zn·$CHCl_3$: C, 59.63; H, 3.49; N, 11.43; Found C, 59.77; H, 4.02; N, 10.46.

(α,α,α,α)-5,10,15,20-Tetrakis(2-(4-fluorophenylurea)phenyl)porphyrin (4). Yield, 80%; mp 240 °C, dec; UV/vis (CH_2Cl_2) λ max (lnϵ): 424 (11.98), 518 (9.12), 553 (9.24), 593 (8.07); ^{1}H NMR δ −2.63 (br s, 2H) 6.57−6.62 (m, 8H), 6.89−6.92 (m, 8H), 7.52 (br s 4H) 7.54 (t, 4H, J = 7.65 Hz), 7.82−8.05 (m, 8H), 8.35 (d, 4H, J = 8.4 Hz), 8.36 (br s 4H), 8.78 (s, 8H); ^{13}C NMR δ 115.21, 115.50, 116.17, 119.78, 122.30, 122.78, 129.56, 131.76, 132.45, 135.86, 139.16, 153.04, 155.85, 159.01; HRFAB MS *mz* calcd for $C_{72}H_{50}N_{12}O_4F_4$ 1223.4092, found 1223.4054 (M + 1); Anal. Calcd for $C_{72}H_{50}N_{12}O_4F_4$·0.5$CHCl_3$: C, 67.87; H, 3.96; N, 13.10. Found C, 68.52; H, 3.79; N, 12.58.

Zn(II) (α,α,α,α)-5,10,15,20-tetrakis(2-(4-fluorophenylurea)phenyl)porphyrin (8). Yield, 95%; mp 230−233 °C; UV/vis (CH_2Cl_2) λ max (lnϵ): 429 (12.09), 559 (9.05), 594 (67.50); ^{1}H NMR δ 6.54−6.60 (m; 8H), 6.74−6.76 (m, 8H), 7.34 (br s, 4H), 7.38 (t, 4H, J = 7.08 Hz) 7.70−7.87 (m, 8H), 8.47 (d, 4H, J = 8.7 Hz), 8.65 (s, 8H), 8.80 (br s 4H); HRFAB MS *mz* calcd for $C_{72}H_{48}N_{12}O_4F_4$.Zn 1285.3227, found 1285.3269 (M + 1); Anal. Calcd for $C_{72}H_{48}N_{12}O_4F_4$·Zn·$CHCl_3$: C, 62.36; H, 3.51; N, 11.95. Found C, 62.80; H, 3.32; N, 10.88.

(α,α,α,α)-5,10,15,20-Tetrakis(2-(4-nitrophenylurea)phenyl)porphyrin (5). Yield, 78%; mp 225−229 °C; UV/vis: CH_2Cl_2 λ max (lnϵ): 423 (11.87), 515 (9.59), 585 (8.50), 640 (7.51); ^{1}H NMR δ −1.3 (s, 2H), 7.06−7.11 (m, 16H), 7.4 (t, 4H, J = 6.84 Hz), 7.70−7.82 (m, 8H), 8.1 (s, br, 4H), 8.36 (d, 4H, J = 8.25 Hz), 8.78 (s, 8H), 9.08 (br s 4H); ^{13}C NMR δ 115.88, 117.33, 118.53, 122.18, 122.56, 125.082, 125.60, 129.69, 132.2, 135.8, 139.25, 141.24, 146.24 152.46, 175.1; HRFAB MS *mz* calcd for $C_{72}H_{50}N_{16}O_{12}$. 1331.3872, found 1331.3850 (M + 1); Anal. Calcd for $C_{72}H_{50}N_{16}O_{12}$·$CHCl_3$: C, 60.44; H, 3.54; N, 15.44. Found C, 60.66; H, 3.86; N, 14.38.

(29) The process is based on an adaptation of the DIFABS[30] logic to area detector geometry by Karaulov: Karaulov, A. I. School of Chemistry and Applied Chemistry, University of Wales, College of Cardiff, Cardiff CF1 3TB, U.K., personal communication.

(30) Walker, N. P.; Stuart, D. *Acta Crystallogr., Sect. A* **1983**, *A39*, 158.

Acknowledgment. D.H.B. wishes to gratefully acknowledge the support of this work by the National Science Foundation (EPS-9550487), and W.R.S. wishes to gratefully acknowledge the support of this work by the NIH (GM-28401).

Supporting Information Available: Figures S1 and S2 presenting additional views of **7**·5DMSO, Figures S3 and S4 giving side views of **3** + TBABr·5DMSO and **3** + TBACl·5DMSO, respectively, and Figures S5 and S6 giving ORTEP diagrams for the **3** + TBABr·3DMSO solvate, Tables S1−S24 with complete crystallographic details, atomic coordinates, anisotropic temperature factors, fixed hydrogen atom positions, bond distances, and bond angles for **7**·5DMSO, **3** + TBABr·5DMSO, **3** + TBACl·5DMSO, and **3** + TBABr·3DMSO (107 pages, print/PDF). See any current masthead page for ordering information and Web access instructions.

JA982052I